Synthesis of Substituted Oxo-Azepines by Regio- and Diastereoselective Hydroxylation

Harold Spedding, Peter Karuso [ID] **and Fei Liu *** [ID]

Department of Molecular Sciences, Macquarie University, Sydney, NSW 2109, Australia;
harold.spedding@hdr.mq.edu.au (H.S.); peter.karuso@mq.edu.au (P.K.)
***** Correspondence: fei.liu@mq.edu.au; Tel.: +61-2-9850-8312

Abstract: Substituted seven-membered *N*-heterocycles are prevalent bioactive epitopes and useful synthons for preparing enzyme inhibitors or molecular recognition systems. To fully exploit the chemical properties of this flexible *N*-heterocycle scaffold, efficient methods for its diverse functionalization are required. Here we utilize the late-stage oxidation of tetrahydroazepines as an approach to access densely functionalized oxo-azepines in a total of 8 steps and ~30% overall yield from commercially available starting materials. Hydroboration of tetrahydroazepines proceeded with diastereoselectivity in a substrate-dependent manner to yield regioisomeric azepanols before their oxidation to the corresponding oxo-azepines. Regioselectivity of the hydroboration step may be improved moderately by a rhodium catalyst, albeit with loss of conversion to a competing hydrogenation pathway. Overall our method allows efficient access to azepanols and oxo-azepines as versatile epitopes and synthons with a high degree of diastereoselectivity and moderate regioselectivity.

Keywords: azepines; hydroboration; diastereoselectivity; oxo-azepines; DFT

1. Introduction

The seven-membered, *N*-heterocyclic azepane scaffold is a biologically active epitope and useful building block in the construction of novel glycosidase inhibitors [1–5], anticancers [6–10], antidiabetics [11–15], antivirals [16,17] and DNA minor groove-binding agents [18–20]. In particular, azepanols and oxo-azepines have received much recent attention as useful epitopes in both materials and medicinal chemistry due to the unique flexibility of the seven-membered ring and resultant spatial distribution of oxygen substituents. For example (Scheme 1a), 2-oxo-azepine **i** reported by Psarra et al. in 2016 exhibited a selective 78% inhibition of TAK1 kinase activity versus other kinase targets, while its constitutional isomer **ii** exhibited comparatively modest and non-selective inhibition of TAK1 activity (58%) [21]. Oxo-azepine **i** may now serve as a scaffold for a detailed structure-activity relationship (SAR) study towards optimized TAK1 inhibition. Pellegrino et al. enantioselectively synthesized and incorporated oxo-azepine **iii** into a tetrapeptide to induce a 3_{10} helical turn into the molecule, as confirmed by NMR and molecular dynamics [22]. This 3_{10} helical conformation was found to be stabilized by key intramolecular hydrogen bonds between the 2-oxo-azepine ketone oxygen and amino acid residues [22,23]. Vankar et al. in 2014 reported *syn*-dihydroxyazepane **iv** as a potent and selective inhibitor of jack bean α-mannosidase, while its epimer **v** was two orders of magnitude less active towards this enzyme [2]. In a recent landmark example, Spiegel et al. prepared glucosepane enantioselectively from oxo-azepine **vi**, yielding a guanidine-containing oxo-azepine (Scheme 1b) [24]. Collectively, these examples highlight the importance of stereochemically well-defined and highly functionalized azepanols and oxo-azepines as biologically active epitopes and synthons. These examples also highlight the need for efficient synthetic methods to access these molecules with regio- and diastereocontrol.

Azepanols and oxo-azepines are typically constructed via the ring-expansion or cyclization of appropriately derivatized sugars or furans with pre-established substitution patterns and stereochemistry. Methods of ring-expansion and cyclization have most-commonly included reductive amination [19,20,25–29] or epoxide ring opening with suitable amines [30,31], ring-closing metathesis (RCM) [32–34], alkene–nitrone cycloaddition [35] and tandem Staudinger aza–Wittig reactions [36]. The Spiegel synthesis of glucosepane utilized commercially available diacetone-D-glucose ($3.20/g) as a precursor to oxo-azepine **vi** via a key Amadori rearrangement (Scheme 1b) [24]. Oxo-azepine **vi** was then further elaborated via the C3-ketone with a sigmatropic rearrangement and cyclization sequence to yield glucosepane in a total of 13 steps and 12% overall yield from diacetone-D-glucose [24]. As part of our work on densely functionalized and conformationally diverse azepanes, we have sought to develop a more-concise route to access oxo-azepines via a late-stage oxidation of tetrahydroazepines [37,38]. Here we report the diastereoselective synthesis of useful oxo-azepine synthons that can be incorporated into complex oxo-azepines such as the glucosepanes (Scheme 1c).
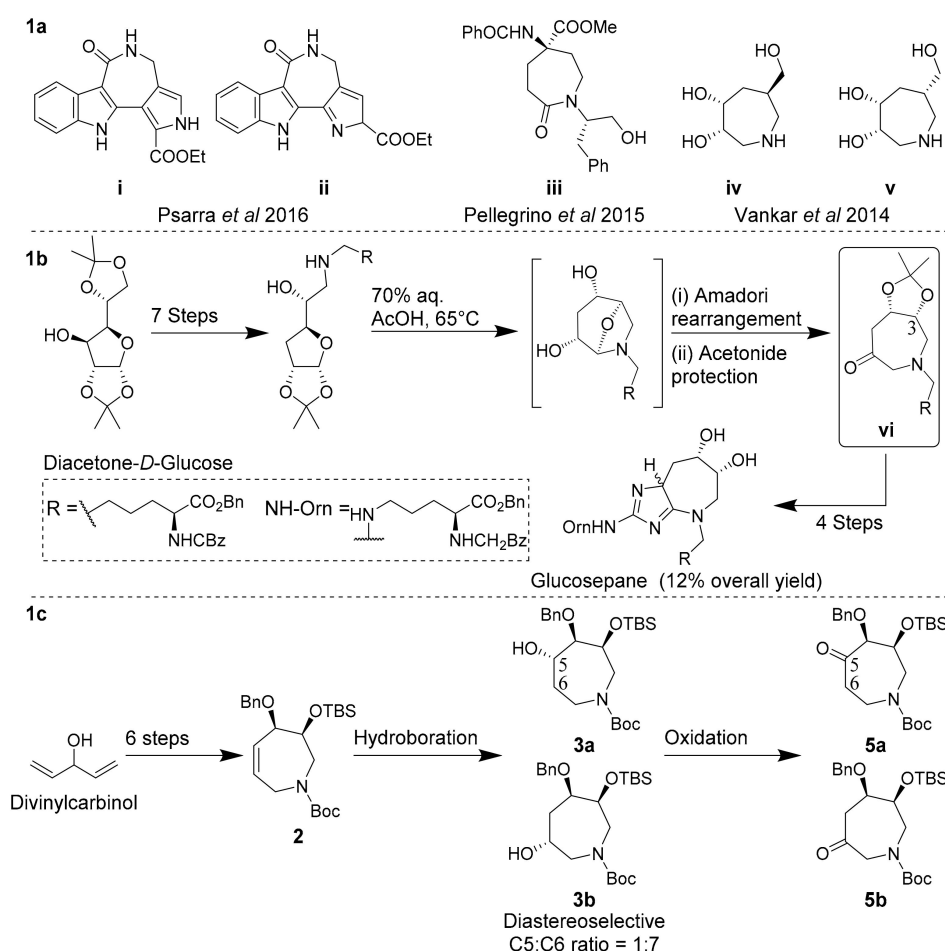
Scheme 1. (**a**) Representative oxo-azepines as glycosidase inhibitors; (**b**) Concise, enantioselective synthesis of glucosepane by Spiegel et al. [24]; (**c**) Current work.

Our previous work showed that hydroboration of the (3*S*)-azido-(4*R*)-tetrahydroazepine proceeded in low regio- and diastereoselectivity [37–39]. Herein, we investigate regio- and diastereoselectivity in the hydroboration of a related tetrahydroazepine **2** (Scheme 1c). Standard and catalytic hydroboration reactions yielded a mixture of the expected (5*S*) and (6*R*) alcohols **3a** and **3b**, respectively, with complete diastereofacial selectivity and moderate regioselectivity. These azepanols were then converted to the corresponding oxo-azepines **5a** and **5b** by oxidation. Overall, the current work with tetrahydroazepine **2** constitutes an efficient and shorter route (8 steps from commercially

available simple starting material) to azepanols and oxo-azepines that can be used as synthons for complex oxo-azepines such as the glucosepanes (13 steps, 12% overall yield).

2. Results

### 2.1. Synthesis of Silyl Ether **2**

Tetrahydroazepine starting material **1** was synthesized from commercially available divinylcarbinol using a concise, 5-step protocol described by Fürstner et al. in 77% overall yield [32]. Silyl ether **2** was then produced in 90% yield using Corey's TBSOTf conditions over 2 h at −80 °C (Scheme 2, conditions (a)) [40]. The same reaction conducted at −20 °C led to *N*-Boc deprotection of **1** and to the formation of *O,N*-TBS protected species **2a** according to preliminary NMR spectroscopic data (Scheme 2, conditions (b)). Compound **2a** appears to degrade by *N*-TBS hydrolysis over several days at −20 °C. The use of Corey's conditions with TBSCl and imidazole in DMF resulted in long reaction times and poor yields for our sterically congested substrate **1** (Scheme 2, conditions (c)), with only 30% conversion to **2** after 48 h at 35 °C [41].
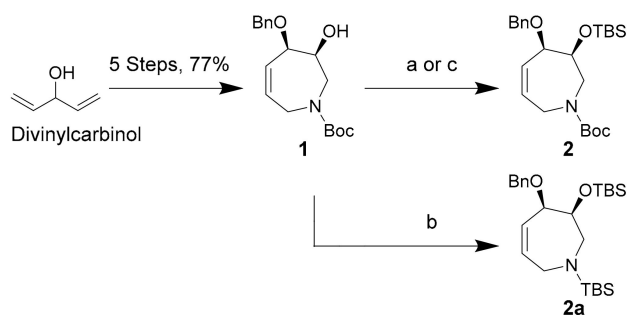
Scheme 2. Silyl-protection conditions for secondary alcohol **1**. Conditions (a) TBSOTf (1.0 equiv), 2,6-lutidine (1.2 equiv), −80 °C, DCM, 2 h, 90%; (b) TBSOTf (1.0 equiv), 2,6-lutidine (1.2 equiv), −20 °C, DCM, 2 h, 50% (of **2a**); (c) TBSCl (3.0 equiv), imidazole (3.5 equiv), 35 °C, DMF, 24 h, 30%.

### 2.2. Hydroboration of (3S)-OTBS Tetrahydroazepine **2**

Hydroboration of tetrahydroazepine **2** proceeded smoothly to yield a 3:2 mixture of regioisomers **3a** and **3b** with excellent diastereofacial selectivity and high yield utilizing borane dimethylsulfide (BH$_3$·SMe$_2$) (Scheme 3). These compounds were isolated by semi-preparative reverse-phase HPLC using acetonitrile:water:trifluoroacetic acid (TFA) (from 50:50:0.1 to 80:20:0.1 over 45 min; flow rate: 4.18 mL/min) as the mobile phase. Separated regioisomers **3a** and **3b** were de-protected to yield azepanols **(5S)-4a** and **(6R)-4b** for characterization by 2D-NMR in the absence of *N*-Boc rotamers.
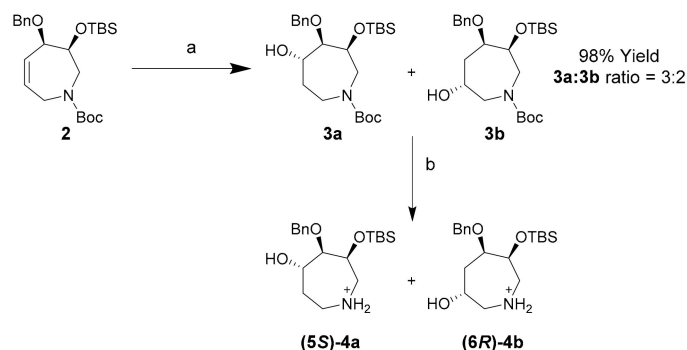
Scheme 3. Synthesis of azepanols **3a** and **3b** and their deprotected derivatives **(5S)-4a** and **(6R)-4b**. Conditions (a) (i) BH$_3$·SMe$_2$, THF, r.t., 1 h; (ii) NaOH, H$_2$O$_2$, EtOH, 80 °C, 1 h, 92%; (b) TFA, r.t., 5 min, 99%.

2.3. Structural Assignment of (5S)-4a and (6R)-4b

Key 2D-NMR correlations (Figure 1) were used to completely assign the ^{1}H and ^{13}C resonances (see Supplementary Materials). Briefly for **(5S)-4a**, an HMBC correlation between C1' (δ_C 74.0 ppm) and H4 (δ_H 3.55 ppm), in combination with an HSQC correlation between H4 and C4 (δ_C 85.6 ppm) was used to identify C4/H4. COSY correlations and HSQCs were then used to assign the rest of the azepine ring (Table S1). NOESY correlations between H4/H6α and H4/H2α allowed stereochemical assignment of H6 and H2 protons. The presence of a strong nOe correlation between H5 and H6β and the absence of nOe correlations between H5 and H3 or H2α suggested 5S stereochemistry at the site of hydroxylation. To further substantiate this hypothesis, compound **(5S)-4a** was synthesized by oxidation of **(5S)-4a** to the 5-ketone **5a**, followed by reduction to a mixture of **(5S)-4a** and **(5S)-4a**. A **(5S)-4a**:**(5R)-4a** ratio of 4:1 was observed for this reduction, likely due to the steric bulk of the *re* face of the azepine ring leading to the observed diastereofacial selectivity in the hydroboration reaction. For **(5R)-4a**, nOe correlations from H5 to H4 and H7α and an absence of nOe correlations between H5 and H7β (Table S2) suggested 5R stereochemistry for the minor component, but the NMR data was far from convincing due to overlapping peaks, especially for the C2 and C7 protons. DFT calculations (next section) were used to substantiate the stereochemical assignments.
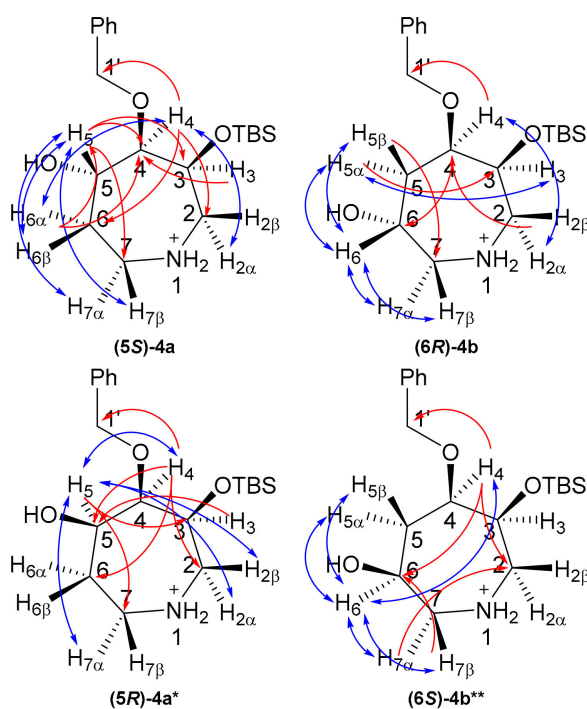
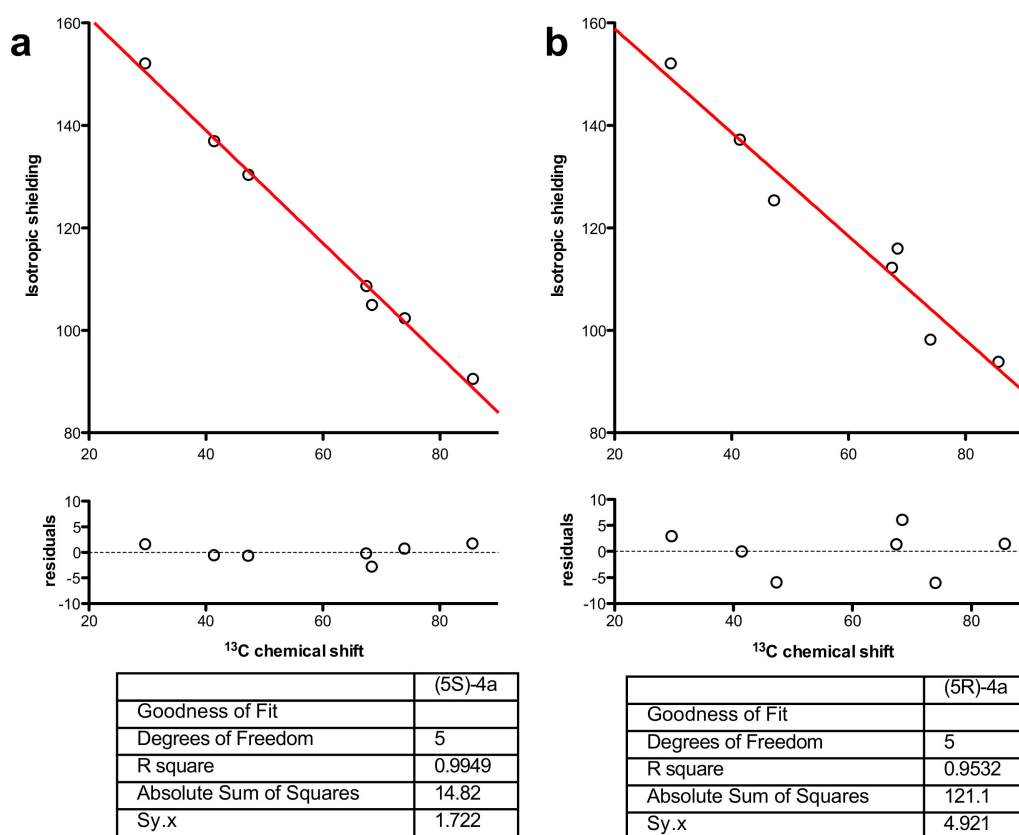**Figure 1.** 2D-NMR correlations for azepanols **(5S)-4a** and **(6R)-4b**. Red, HMBC; blue, NOESY. * Characterized as a mixture with **(5S)-4a**; ** Characterized as a mixture with **(6R)-4b**.

Compound **(6R)-4b** was characterized by the same approach. The combination of an HMBC between C1' (δ_C 72.5 ppm) and H4 (δ_H 3.84 ppm), and an HSQC between H4 and C4 (δ_C 77.5 ppm) was used to identify C4/H4. COSY correlations and HSQCs were used to identify the remainder of the azepine ring and site of hydroxylation (C6; 63.7 ppm, Table S3). The 6R stereochemistry of **(6R)-4b** was supported by strong nOe correlations from H6 to H5α, H5β, H7α and H7β. This suggested that H6 is synclinal to H5α, H5β, H7α and H7β, but this could not be used to confirm the stereochemistry. Similarly, the absence of nOe correlations from H6 to H2α, H3 and H4 was weak evidence of **6R** stereochemistry. To help with the assignment, a mixture of **(6R)-4b** and **(6S)-4b** was synthesized using the same oxidation/reduction approach as for **4a** (Table S4). In compound **(6S)-4b**, H6 showed

stronger nOe correlations to H5α and H7α than to H5β and H7β, consistent with a β-OH and thus 6*S* stereochemistry for this compound and in support of 6*R* stereochemistry for **4b**.

### 2.4. DFT Analysis of **(5S)-4a** and **(5R)-4a**

Models of **(5S)-4a** and **(5R)-4a** were built in MOE (Molecular Operating Environment) [42], and a conformational search using low-mode molecular dynamics was made from each structure and the remaining azepine geometry using the MMFF94x force-field for minimization. The TBS and Ph groups were then stripped from the structures and the remaining azepines' geometry optimized using Turbomole 7.1 (DFT//BP86/SV(P) then DFT//B3-LYP/def2-TZVPP) [43]. The NMR shielding constants were then calculated at the same level of theory (DFT//B3-LYP/def2-TZVPP) and plotted against the actual ^{13}C- and ^{1}H-NMR data of **(5S)-4a** and **(5R)-4a** (see Supplementary Materials). Non-linear least-squares fitting to a straight line (GraphPad Prism 5.0) resulted in a goodness of fit (R; Figure 2).

	(5S)-4a
Goodness of Fit	
Degrees of Freedom	5
R square	0.9949
Absolute Sum of Squares	14.82
Sy.x	1.722

	(5R)-4a
Goodness of Fit	
Degrees of Freedom	5
R square	0.9532
Absolute Sum of Squares	121.1
Sy.x	4.921

Figure 2. Non-linear regression fitted to a straight line of chemical shifts against calculated isotropic shielding (DFT//B3-LYP/TZVPP) for (**a**) **(5S)-4a** and (**b**) **(5R)-4a** with residuals and goodness-of-fit values.

Non-linear regression showed a better fit for ^{13}C-NMR chemical shifts for **(5S)-4a** (Figure 2a) than for **(5R)-4a**, whereas the lowest-energy structure gave a poorer fit (R^2 = 0.9532 vs. 0.9949) with several ^{13}C resonances (notably C5 and the benzylic carbon) greater than 5 ppm from the line of best fit (Figure 2b). In light of this regression analysis and experimental spectral data for **4a**, we conclude that the molecule has, on the weight of evidence, 5*S* stereochemistry. Finally, it is noteworthy that the DFT calculations predict a conformation (Figure 3) where H5 would not show any diagnostic nOes to H3 and H2α. Similarly, the minimum-energy structure for **(6R)-4b** (Figure 3, right) showed that H5 is synclinal to H5α, H5β, H7α and H7β, and that H5 would indeed not be expected to show nOe

correlations to H2α, H3 or H4 and nOes of roughly equal intensity to H5α, H5β, H7α and H7β, as is observed (see Supplementary Materials).
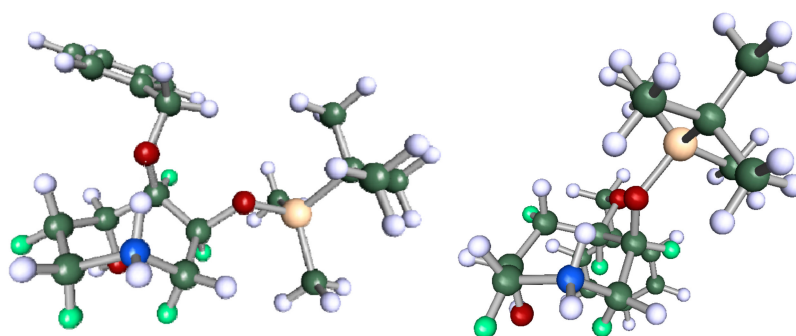

Figure 3. Global lowest-energy structure of **(5S)-4a** (**left**) and **(6R)-4b** (**right**), α-protons coloured green.

2.5. Reagent and Catalyst Screen for the Hydroboration of **2**

The stereochemical and regiochemical outcomes of hydroborations of substituted alkenes is related to the steric and stereoelectronic environment of both the reagent and substrate. In this case, the hydroboration of (3*R*)-OTBS tetrahydroazepine **2** using BH$_3$·SMe$_2$ proceeded with excellent diastereofacial selectivity but low regioselectivity to provide **3a** and **3b**. In contrast, hydroboration of a (3*S*)-azidotetrahydroazepine in our earlier work proceeded with low diastereo- and regioselectivity, yielding all four possible C5/C6 azepanols (product ratio 5*S*:5*R*:6*S*:6*R* = 1:36:32:28) [39]. It is likely that the bulky (3*R*)-OTBS group, along with the other substituents of tetrahydroazepine **2**, present significant steric bias to the cyclic alkene that was absent in the (3*S*)-azido substrate. We were thus interested in screening reagents and catalysts to explore potential regioselectivity in the hydroboration of substrate **2** (Scheme 4).

Hydroboration of **2** with a variety of common borylating reagents (Table 1) proceeded with poor or no yield of the azepanols (Table 1, Entries 2–7) except for BH$_3$·SMe$_2$ (Table 1, Entry 1). The use of more-stable borylating reagents, including catechol borane, pinacol borane and 9-BBN, yielded no azepanol product upon oxidation, even when borylation was conducted in refluxing THF. In the case of catechol borane, the addition of Wilkinson's catalyst (Table 1, Entry 5) resulted exclusively in the formation of hydrogenation product **3e**.
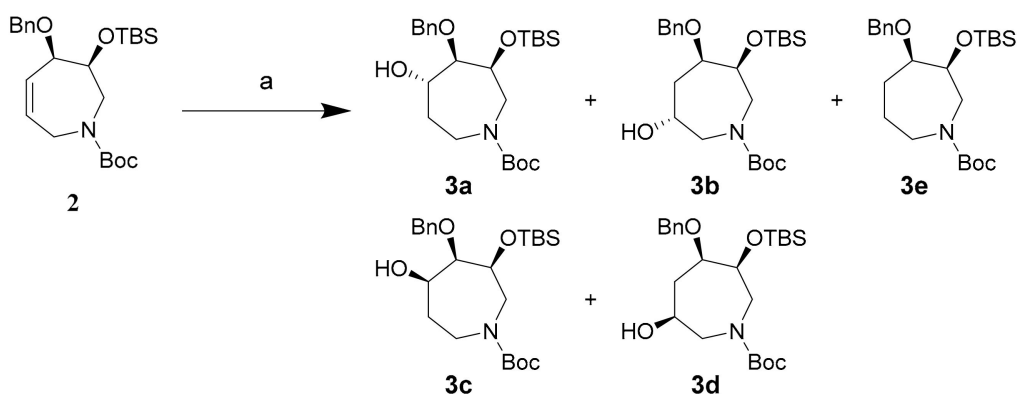
Scheme 4. Reagent and catalyst screen for the hydroboration of **2**. Conditions (a) (i) BHR$_2$, see Table 2, THF; (ii) NaOH, H$_2$O$_2$, EtOH, 80 °C, 1 h, 99%.

Table 1. Screening of different hydroboration reagents.

Entry	Conditions	Conversion (%)	Ratio [c]		
			3a	**3b**	**3e**
1	BH$_3$·SMe$_2$, 25 °C, 18 h	99	58	42	0
2	BH$_3$·THF, 25 °C, 18 h	4.3 [b]	69	31	0
3	BH$_3$·NMe$_3$, 66 °C, 18 h	0 [b]	0	0	0
4	CatBH, 66 °C, 18 h	0 [b]	0	0	0
5 [a]	CatBH, 66 °C, 18 h	100	0	0	100
6	9-BBN, 66 °C, 18 h	0 [b]	0	0	0
7	PinBH, 25 °C, 18 h	0 [b]	0	0	0

[a] 10 mol % Wilkinson's catalyst was added. [b] Starting material was recovered. [c] All reactions were carried out in THF with product ratios determined by HPLC. Formation of **3c** and **3d** was not observed.

Transition-metal catalysts for hydroborations have been shown to exhibit remarkable chemo- [44], regio- [45] and stereoselectivities [44,46–49] for a variety of acyclic and cyclic substrates [44,50–53]. We screened a variety of catalysts for the hydroboration of tetrahydroazepine **2** (Table 2). Use of iridium and rhodium catalysts led to the formation of hydrogenation product **3e** as the major product (Table 2, Entries 1–3). This suggests the addition of our densely functionalized substrate, **2**, to the metal centre is slow, as expected for unreactive olefins [54,55]. Loading of **2** is likely out-competed by diboration of the metal centre with accompanying hydrogen release that leads to formation of **3e** in the presence of the metal catalyst [54,55].

Due to the difficulty in isolating hydrogenation product **3e** from starting material **2** by semi-preparative LC, **3e** was formed directly by hydrogenation of compound **2**. The ^{1}H-NMR spectrum of compound **3e** was then compared with crude reaction mixtures (Table 2, Entries 1–2) to verify its formation under catalytic hydroboration conditions (for chromatograms, see Supplementary Materials). Compound **3e** was deprotected to yield **4c** and characterized by 2D-NMR in the absence of *N*-Boc rotamers (Table S5).

In the case of PinBH with Rh(COD)(DPPB)BF$_4$, modest conversion to the desired azepanol products was observed with a considerable bias towards the 6*R* regioisomer **3b** while preserving the diastereoselectivity (Table 2, Entry 2). Improved regioselectivity may be accounted for by borylation at the most sterically accessible position, as is observed with other OTBS-protected substrates. This steric effect appears to outweigh any potential directed borylation via the allylic OBn group to the *syn* face of the substrate. Addition of the Lewis acid additive tris(pentafluorophenyl)borane (FAB), as reported by Lata and Crudden [56], increased the formation of **3e** without improving the regioselectivity between **3a** and **3b** (Table 2, Entry 3). The use of a copper (I) metal centre with TangPhos (Table 2, Entry 4) and bulky (*R*)-DTBM SegPhos (Table 2, Entry 5) ligands resulted in no formation of any product [57,58].

Table 2. Catalyst screen for the hydroboration of **2**.

Entry	Conditions	Conversion (%)	Ratio [b]		
			3a	**3b**	**3e**
1	CatBH, 5 mol % Ir(COD)(PCy$_3$)(Py)PF$_6$, THF, 66 °C, 18 h	44 [a]	0	0	100
2	PinBH, 5 mol % Rh(COD)(DPPB)BF$_4$, DCE, 25 °C, 18 h	75 [a]	5	34	61
3	PinBH, 5 mol % Rh(COD)(DPPB)BF$_4$, 2 mol % FAB, DCE, 66 °C, 18 h	58 [a]	2	8	90
4	PinBH, 3 mol % CuCl, 3.3 mol % TangPhos, 6 mol % NaO^{t}Bu, toluene, 66 °C, 18 h	0 [a]	0	0	0
5	PinBH, 3 mol % CuCl, 3.3 mol % (*R*)-DTBM SegPhos, 6 mol % NaO^{t}Bu, toluene, 66 °C, 18 h	0 [a]	0	0	0

[a] Starting material was recovered. [b] No **3c** or **3d** was formed in these reactions.

In contrast to neutral rhodium catalysts for hydroboration, rhodium (I) catalysts exhibit marked solvent-dependent variations in yield, stereo- and regioselectivity for a variety of substrates [52,54,55]. In an attempt to optimize the hydroboration of **2** with PinBH/5 mol % Rh(COD)(DPPB)BF$_4$, the most-active catalyst for the substrate, a solvent screen was conducted (Table 3). In the relatively

high-polarity solvent DCE at 60 °C, hydroboration proceeded with good conversion and suppression of the hydrogenation product **3e** (Table 3, Entry 1) compared to the same reaction at ambient temperature (Table 2, Entry 2). This reaction also proceeded with comparable diastereoselectivity and an increase in regioselectivity (Table 3, Entry 1, **3a**:**3b** = 1:8) in favour of **3b** as the kinetic product compared to the same reaction at ambient temperature (Table 2, Entry 2, **3a**:**3b** = 1:7).

Table 3. Solvent screen for the hydroboration of **2** using PinBH and 5–10 mol % Rh(COD)(DPPB)BF$_4$.

| Entry	Conditions	Conversion (%)	Ratio [b]		
			3a	**3b**	**3e**
1	DCE, 60 °C, 18 h	70	7	54	39
2 [a]	DCE, 60 °C, 18 h	37	3	14	83
3	THF, 25 °C, 18 h	99	8	48	44
4	THF, 60 °C, 18 h	99	8	58	34
5	Toluene, 25 °C, 18 h	98	5	39	56
6	Toluene, 60 °C, 18 h	100	6	44	50
7 [a]	Toluene, 60 °C, 18 h	44	11	57	32

[a] 1 mol % catalyst loading. [b] No **3c** or **3d** was formed in these reactions.

In THF and toluene, the reaction proceeded with the highest regioselectivity (**3a**:**3b** = 1:8, Table 3, Entry 5) in favour of **3b** with similarly high conversion upon heating (Table 3, Entries 4 and 6). In these solvents, THF exhibited the least formation of hydrogenation product **3e**, while toluene exhibited the most. Considering that DCE and toluene, the most- and least-polar of the solvents screened, respectively, had comparable amounts of hydrogenation product **3e**, the formation of **3e** does not appear to be dependent on solvent polarity. It may be possible, then, that the ability of THF to coordinate the borane and metal centre precludes diboration of the metal centre and therefore mildly suppresses formation of **3e**. In addition, reduction of the catalyst loading from 5–10 mol % to 1 mol % in DCE (Table 3, Entry 2) increased the proportion of **3e** formed, suggesting borane addition to the metal centre effectively out-competes alkene addition. In toluene (Table 3, Entry 7), reduction of the catalyst loading in the same manner yielded an 18% decrease in the amount of **3e** formed, although conversion was still poor over 18 h. In summary, hydrogenation is competitive with hydroboration of our very sterically congested azepane substrate **2**. As a compromise between conversion, regioselectivity and suppression of **3e** formation, the optimal conditions for the catalytic hydroboration of **2** with PinBH/5 mol % Rh(COD)(DPPB)BF$_4$ is THF at 60 °C (Table 3, Entry 4). These conditions facilitate nearly complete conversion of substrate **2** to azepanol regioisomers **3a** and **3b** in a ratio of 1:7, with minimal formation of hydrogenation product **3e**.

*2.6. Synthesis and Structural Assignment of (3R)-OTBS-5/6-Oxo-Azepines **5a** and **5b***

Oxidation of crude **3a**/**3b** azepanol mix using pyridinium chlorochromate proceeded to completion in 1 h, however in modest yield of oxo-azepines **5a** and **5b** (Scheme 5). Hydration of these products during work-up resulted in loss during column chromatography on Celite and silica gel. This problem was circumvented using dried 4Å molecular sieves (MS) for work-up, improving the combined isolated yield of **5a** and **5b** to 75%. *N*-Boc deprotected derivatives **6a** and **6b** were characterized by 2D-NMR spectroscopy.
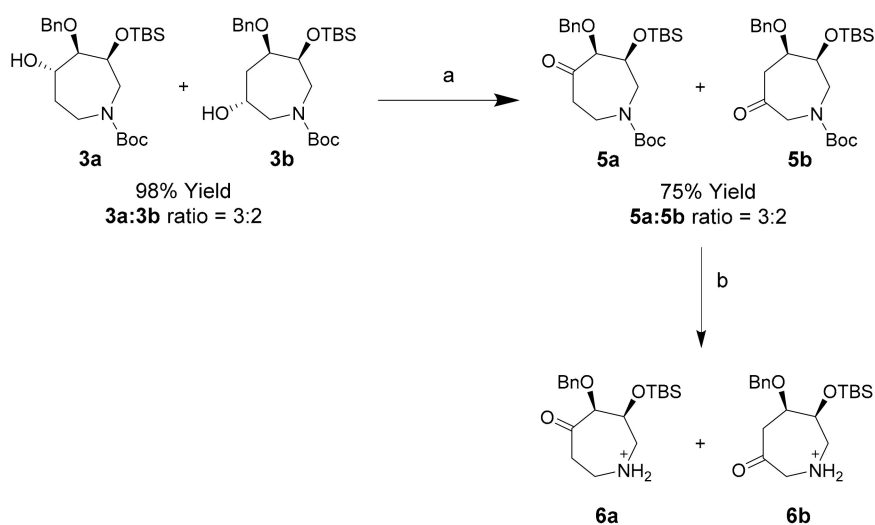
Scheme 5. Synthesis of oxo-azepines **5a** and **5b** and their *N*-Boc deprotected counterparts **6a** and **6b**. Conditions (a) PCC, DCM, 25 °C, 45 min, 75%; (b) TFA, r.t., 5 min, 99%.

In comparison to azepanols **(5S)-4a** and **(6R)-4b**, structural assignment of ketones **6a** (Table S6) and **6b** (Table S7) is considerably less ambiguous in the absence of the monoalcohol stereocentre. These ketones, with their characteristic carbonyl ^{13}C chemical shift, can be assigned directly from HMBC correlations and indirectly by a combination of COSY and HSQC correlations. In addition, the stereoelectronic bias exerted by the ketone reduces the conformational freedom of the ring, enhancing observed COSY and NOESY correlations (Figure 4).
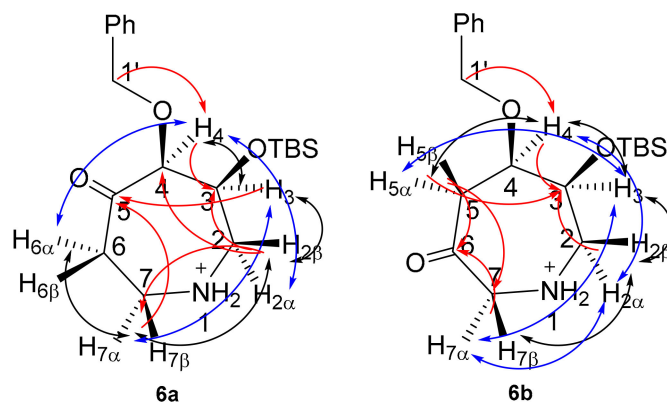
Figure 4. 2D-NMR correlations for monohydroxyl azepanes **6a** and **6b**. Red, HMBC; black, COSY; blue, NOESY.

For **6a**, an HMBC between H1′ (δ_H 4.47, 4.85 ppm) and C4 (δ_C 87.2 ppm), combined with an HSQC between C4 and H4 (δ_H 4.32 ppm), was used to identify C4 (Table S6). In the same manner, COSY and HSQC correlations were used to assign the rest of the azepine ring (Table S6). Strong HMBC correlations from C5 (δ_C 202.1 ppm) to H3, H7α and H7β were used to identify the ketone at C5.

For **6b**, an HMBC between H1′ (δ_H 4.67 ppm) and C4 (δ_C 75.5 ppm), combined with an HSQC between C4 and H4 (δ_H 3.84 ppm), was used to identify C4. COSY correlations and HSQC were then used to assign the rest of the azepine ring (Table S7). A strong $^3J_{CH}$ correlation from H4 to C6 (δ_C 200.5 ppm) and $^2J_{CH}$ correlations from H5α, H5β, H7α and H7β to C6 were used to identify the ketone at C6. Stereospecific proton assignments were based on nOe correlations (Tables S6 and S7).

3. Materials and Methods

3.1. General Methods

All reagents were purchased from Sigma-Aldrich and used without further purification. Dichloromethane (DCM) and tetrahydrofuran (THF) were distilled from calcium hydride. All reactions were conducted in flame-dried glassware and under nitrogen atmosphere unless stated otherwise. All reactions were magnetically stirred and monitored by thin-layer chromatography (TLC) using Merck silica gel 60 F_{254} pre-coated plates (0.25 mm). Flash column chromatography was performed using silica gel (0.032–0.063 mm particle size) from Fisher Scientific. All ^{1}H-, ^{13}C- and 2D-NMR experiments were performed on either a Bruker Avance DPX 400 MHz, Bruker Avance III HD NanoBay 400 MHz or DRX600 NMR spectrometer equipped with a TXI (5 mm) cryoprobe. Chemical shifts were reported in ppm using residual $CDCl_3$ (δ_H; 7.26 ppm, δ_C; 77.36 ppm), or $(CD_3)_2CO$ (δ_H; 2.05 ppm, δ_C; 29.84 ppm), or CD_3OD (δ_H; 3.31 ppm, δ_C; 49.00 ppm) as an internal reference. Polarimetry data was collected on a JASCO polarimeter (model no. P-1010). LC–MS was conducted using an Agilent 6130 single-quadrupole LC–MS system. High-resolution mass-spectrometry (HRMS) was conducted using a Thermo-Fisher QExactive-Plus Orbitrap instrument. Infrared spectroscopy was conducted using a Thermo-Fisher Nicolet iS5 FT–IR spectrometer.

3.2. Synthetic Procedures

3.2.1. *tert*-Butyl(3*S*,4*R*)-4-(benzyloxy)-3-((*tert*-butyldimethylsilyl)oxy)-2,3,4,7-tetrahydro-1*H*-azepine-1-carboxylate (**2**)

To a stirred solution of tetrahydroazepanol **1** (0.571 g, 1.8 mmol) in dry DCM (8.9 mL) at −40 °C was added successively 2,6-lutidine (0.497 mL, 4.3 mmol) and *tert*-butyldimethylsilyl trifluoromethanesulfonate (0.822 mL, 2.1 mmol). The reaction proceeded at the same temperature for 40 min until completion according to TLC before being quenched by the addition of H_2O. The organic layer was extracted twice with DCM, dried with $MgSO_4$ and concentrated in vacuo. Crude residue was purified by flash chromatography (petroleum ether/ethyl acetate 9:1) to yield **2** as a clear, light yellow oil (90%). $[\alpha]_D^{20}$ −43 (*c* 0.19, $CHCl_3$); FTIR (ATR): 2953, 2929, 1697, 1411, 1245, 1169, 1137, 834, 776 cm^{-1}. ^{1}H-NMR (400 MHz, $CDCl_3$): δ 7.37–7.23 (m, 5H), 5.93–5.62 (m, 2H), 4.67–4.54 (m, 2H), 4.28–4.24 (m, 1H), 4.15–4.06 (m, 1H), 3.99–3.81 (m, 2H), 3.73–3.62 (m, 1H), 3.33–3.23 (m, 1H), 1.41 (s, 9H), 0.89 (s, 5H), 0.87 (s, 4H), 0.07–0.06 (m, 6H). ^{13}C-NMR (150 MHz, $CDCl_3$): δ 138.94, 130.93, 129.43, 128.61, 127.88, 127.76, 78.22, 72.26, 71.60, 51.46, 46.29, 28.76, 26.17, 18.52, −4.2418, −4.50. HRMS–ESI: [M + H]$^+$ calcd. for $C_{24}H_{40}NO_4Si$: 434.2727; found 434.2718.

3.2.2. *tert*-Butyl(3*S*,4*R*,5*S*)-4-(benzyloxy)-3-((*tert*-butyldimethylsilyl)oxy)-5-hydroxyazepane-1-carboxylate (**3a**); *tert*-Butyl(3*S*,4*R*,6*S*)-4-(benzyloxy)-3-((*tert*-butyldimethylsilyl)oxy)-5-hydroxyazepane-1-carboxylate (**3b**)

To a solution of silyl ether **2** (142 mg, 0.33 mmol) in THF (316 μL) at 25 °C and under N_2 atmosphere was added BH_3·SMe_2 (2.0 M in THF, 180 μL, 0.36 mmol) dropwise. The reaction mixture was left to stir at the same temperature for 1 h before sequential addition of ethanol (1.92 mL), 6 M sodium hydroxide (1.44 mL) and 30% H_2O_2 (0.67 mL), followed by heating to 60 °C for 1 h. The reaction was cooled and quenched by the addition of saturated NH_4Cl, after which the layers separated. The aqueous layer was then extracted with ethyl acetate (3 × 5 mL), dried with $MgSO_4$ and rotary evaporated to yield crude alcohols **3a** and **3b** (136 mg, 92% yield) as a pale yellow oil. Crude product was used for PCC oxidation without purification. In addition, preparative HPLC (mobile phase—acetonitrile:water:TFA from 50:50:0.1 to 80:20:0.1 over 45 min; flow rate–4.18 mL/min) was used to isolate regioisomeric alcohols **3a** and **3b** as colourless oils with an overall yield of 92% and **3a:3b** ratio of 3:2.

(**3a**) $[\alpha]_D^{20}$ +19 (*c* 0.02, $CHCl_3$). FTIR (ATR): 2953, 2929, 1671, 1200, 1132, 835, 721 cm^{-1}. ^{1}H-NMR (400 MHz, $CDCl_3$): δ 7.40–7.26 (m, 5H), 4.78–4.70 (m, 1H), 4.55–4.40 (m, 1H), 4.40–4.26 (m, 1H), 4.06–3.96

(m, 1H), 3.80–3.40 (m, 3H), 3.34–3.15 (m, 2H), 2.58 (s, broad, 1H), 2.15–2.00 (m, 1H), 1.70–1.53 (m, 1H), 1.45 (s, 9H), 0.95–0.85 (m, 9H), 0.10–0.05 (m, 6H). ^{13}C-NMR (150 MHz, CDCl$_3$): δ 155.73, 138.05, 128.89, 128.26, 128.19, 86.66, 79.92, 72.86, 69.62, 68.92, 49.46, 41.96, 33.00, 28.79, 26.11, 18.33, −4.29, −4.65. HRMS–ESI: [M + H]$^+$ calcd. for C$_{24}$H$_{42}$NO$_5$Si: 452.2832; found 452.2825.

(**3b**) $[\alpha]_D^{20}$ −25 (*c* 1, CHCl$_3$). FTIR (ATR): 2951, 2929, 1669, 1413, 1250, 1165, 1074, 836, 776 cm^{-1}. ^{1}H-NMR (400 MHz, CDCl$_3$): δ 7.40–7.25 (m, 5H), 4.71 (d, *J* = 12.12 Hz, 1H), 4.62 (d, *J* = 12.08 Hz, 1H), 4.10–3.95 (m, 2H), 3.95–3.73 (m, 4H), 3.47–3.25 (m, 1H), 3.10–2.90 (m, 1H), 2.50–2.30 (m, 1H), 1.62 (s, broad, 1H), 1.47 (s, 9H), 0.91 (s, 9H), 0.08 (s, 6H). ^{13}C-NMR (150 MHz, CDCl$_3$): δ 158.32, 139.28, 128.64, 127.77, 127.67, 80.95, 78.03, 74.72, 73.07, 69.79, 54.87, 51.24, 35.16, 28.74, 26.15, 18.40, −4.36, −4.45. HRMS–ESI: [M + H]$^+$ calcd. for C$_{24}$H$_{42}$NO$_5$Si: 452.2832; found 452.2825.

3.2.3. (3*R*,4*R*,5*S*)-4-(Benzyloxy)-3-((*tert*-butyldimethylsilyl)oxy)-5-hydroxyazepane (**(5*S*)-4a**)

Alcohol **3a** (5.0 mg, 11 μmol) was dissolved in trifluoroacetic acid (TFA, 500 μL) at 25 °C and stirred for 5 min before evaporation of the TFA under N$_2$ flow. Traces of TFA were then removed under high-vacuum (0.01 torr, 25 °C) for 3 h, yielding alcohol **(5*S*)-4a** as a light yellow oil (3.9 mg, quant.). $[\alpha]_D^{20}$ +8 (*c* 0.12, CHCl$_3$). FTIR (ATR): 2953, 2929, 1671, 1200, 1132, 835, 778 cm^{-1}. ^{1}H-NMR (400 MHz, CDCl$_3$): δ 9.95 (s, broad, 1H), 8.45 (s, broad, 1H), 7.29–7.40 (m, 5H), 4.80 (d, *J* = 11.7 Hz, 1H), 4.57 (d, *J* = 11.6 Hz, 1H), 4.42 (dd, *J* = 7.1, 2.8 Hz, 1H), 4.01 (ddd, *J* = 6.8, 6.8, 4.4 Hz, 1H), 3.58 (dd, *J* = 6.8, 1.3 Hz, 1H), 3.32 (m, 1H), 3.29 (m, 2H), 3.28 (s, broad, 1H), 3.16 (m, 1H), 2.26 (dddd, *J* = 15.9, 8.1, 4.3, 3.6 Hz, 1H), 1.92 (dddd, *J* = 15.8, 9.0, 6.5, 2.6 Hz, 1H), 0.89 (s, 9H), 0.11 (s, 3H), 0.09 (s, 3H). ^{13}C-NMR (150 MHz, CDCl$_3$): δ 137.78, 128.98, 128.50, 128.23, 85.62, 73.97, 68.38, 67.41, 47.24, 41.39, 29.60, 25.99, 18.24, −4.50, −4.84. HRMS–ESI: [M]$^+$ calcd. for C$_{19}$H$_{34}$NO$_3$Si: 352.2308; found 352.2300.

3.2.4. (3*R*,4*R*,6*S*)-4-(Benzyloxy)-3-((*tert*-butyldimethylsilyl)oxy)-5-hydroxyazepane (**(6*R*)-4b**)

Alcohol **3b** (5.0 mg, 11 μmol) was *N*-Boc deprotected as above for **3a**, yielding alcohol **(6*R*)-4b** as a pale yellow oil (3.9 mg, quant.). $[\alpha]_D^{20}$ +8 (*c* 0.07, CHCl$_3$); FTIR (ATR): 2953, 2929, 1672, 1199, 1132, 835, 778 cm^{-1}. ^{1}H-NMR (400 MHz, CDCl$_3$): δ 9.50 (s, broad, 1H), 8.42 (s, broad, 1H), 7.37–7.25 (m, 5H), 4.53 (d, *J* = 11.8 Hz, 1H), 4.48 (d, *J* = 11.8 Hz, 1H), 4.26 (m, 1H), 4.21 (m, 1H), 3.84 (dd, *J* = 9.5, 2.3 Hz, 1H), 3.41 (m, 2H), 3.33 (dd, *J* = 13.7, 3.3 Hz, 1H), 3.17 (dd, *J* = 13.3, 5.5 Hz, 1H), 2.26 (dq, *J* = 14.4, 4.8 Hz, 1H), 2.01 (dt, *J* = 14.5, 3.8 Hz, 1H), 0.89 (s, 9H), 0.08–0.06 (m, 6H). ^{13}C-NMR (150 MHz, CDCl$_3$): δ 138.37, 128.75, 128.06, 127.85, 77.48, 72.50, 71.48, 63.69, 50.63, 48.73, 34.63, 26.01, 18.26, −4.37, −4.94. HRMS–ESI: [M + H]$^+$ calcd. for C$_{19}$H$_{34}$NO$_3$Si: 352.2308; found 352.2300.

3.2.5. *tert*-Butyl (3*S*,4*S*)-4-(benzyloxy)-3-((*tert*-butyldimethylsilyl)oxy)-5-oxo-azepine-1-carboxylate (**5a**); *tert*-Butyl (3*S*,4*S*)-4-(benzyloxy)-3-((*tert*-butyldimethylsilyl)oxy)-6-oxo-azepine-1-carboxylate (**5b**)

Pyridinium chlorochromate (PCC, 130 mg, 0.60 mmol) was added to a well-stirred suspension of alcohol diastereomers **3a** and **3b** (91 mg, 0.20 mmol) and 4 Å MS (137 mg) in dry DCM (10 mL) under N$_2$ atmosphere at 25 °C. The reaction mixture was then stirred for 1 h followed by passage through a plug of dry 4 Å MS and flash column chromatography (petroleum ether/ethyl acetate 9:1) to yield pure fractions of **5a** (28.5 mg) and **5b** (40.2 mg) in 75% overall yield.

(**5a**) $[\alpha]_D^{20}$ +11 (*c* 1, CHCl$_3$); FTIR (ATR): 2955, 2929, 1696, 1406, 1159, 1093, 834, 776 cm^{-1}. ^{1}H-NMR (400 MHz, CDCl$_3$): δ 7.40–7.25 (m, 5H), 4.73–4.66 (m, 2H), 4.15–4.05 (m, 1H), 3.95–3.60 (m, 4H), 3.45–3.35 (m, 1H), 2.85–2.55 (m, 2H), 1.43 (s, 9H), 0.91–0.87 (m, 9H), 0.14–0.06 (m, 6H). ^{13}C-NMR (150 MHz, CDCl$_3$): δ 209.71, 154.90, 137.92, 128.83, 128.82, 128.00, 90.98, 80.38, 74.23, 72.36, 50.51, 42.65, 41.84, 28.61, 26.06, 18.35, −4.56, −4.66. HRMS–ESI: [M+H]$^+$ calcd. for C$_{24}$H$_{40}$NO$_5$Si: 450.2676; found 450.2669.

(**5b**) $[\alpha]_D^{20}$ +32 (*c* 1, CHCl$_3$); FTIR (ATR): 2954, 2929, 1697, 1409, 1155, 1109, 1079, 835, 775 cm^{-1}. ^{1}H-NMR (400 MHz, CDCl$_3$): δ 7.40–7.20 (m, 5H), 4.80–4.60 (m, 2H), 4.60–4.20 (m, 1H), 4.10–3.70 (m, 3H), 3.60–3.10 (m, 2H), 2.81 (dd, *J* = 14.36, 8.16 Hz, 1H), 2.6 (dd, *J* = 21.09, 13.93 Hz, 1H), 1.50 (s, 5H), 1.43 (s, 4H), 0.93 (s, 9H), 0.20–0.08 (m, 6H). ^{13}C-NMR (150 MHz, CDCl$_3$): δ 208.93, 155.58, 138.42, 128.66,

127.95, 127.64, 81.28, 76.79, 74.55, 73.06, 59.13, 49.84, 43.74, 28.85, 26.12, 18.35, −4.34, −4.58. HRMS–ESI: $[M + H]^+$ calcd. for $C_{24}H_{40}NO_5Si$: 450.2676; found 450.2668.

3.2.6. (3*S*,4*S*)-4-(Benzyloxy)-3-((*tert*-butyldimethylsilyl)oxy)-5-oxoazepan-1-ium (**6a**)

Ketone **6a** (5.0 mg, 11 μmol) was produced as above for (**5S)-4a** and was isolated as a pale light yellow powder (3.9 mg, 95%). $[\alpha]_D^{20}$ +10 (*c* 1, CHCl₃); FTIR (ATR): 2953, 2930, 1672, 1171, 1132, 835, 781 cm⁻¹. ¹H-NMR (400 MHz, CDCl₃): δ 7.38–7.26 (m, 5H), 4.84 (d, *J* = 11.68 Hz, 1H), 4.47 (d, *J* = 11.68 Hz, 1H), 4.32 (s, broad, 1H), 4.30 (m, 1H), 3.74–3.60 (m, 1 H), 3.50 (dd, *J* = 13.62, 5.98 Hz, 1H), 3.45–3.20 (m, 2H), 2.79 (t, *J* = 4.46, 2H), 0.85 (s, 9H), 0.09 (s, 3H), 0.08 (s, 3H). ¹³C-NMR (150 MHz, CDCl₃): δ 202.10, 137.19, 128.93, 128.28, 128.09, 87.18, 69.93, 51.33, 41.99, 38.29, 25.93, 25.84, 18.24, −4.63, −4.95. HRMS–ESI: $[M + H]^+$ calcd. for $C_{19}H_{32}NO_3Si$: 350.2152; found 350.2142.

3.2.7. (3*S*,4*S*)-4-(Benzyloxy)-3-((*tert*-butyldimethylsilyl)oxy)-6-oxoazepan-1-ium (**6b**)

Ketone **6b** (5.0 mg, 11 μmol) was produced as above for (**5S)-4a** and was isolated as a pale light yellow oil (3.9 mg, 95%). $[\alpha]_D^{20}$ +25 (*c* 1, CHCl₃); FTIR (ATR): 2955, 2929, 1676, 1655, 1175, 1136, 836, 778 cm⁻¹. ¹H-NMR (400 MHz, CDCl₃): δ 7.37–7.26 (m, 5H), 4.67 (s, broad, 2H), 4.32 (m, 1H), 3.84 (m, 1H), 3.68 (d, *J* = 17.92 Hz, 2H), 3.43 (dd, *J* = 13.20, 9.53 Hz, 1H), 3.33 (dd, *J* = 13.20, 3.99 Hz, 1H), 3.13 (dd, *J* = 15.26, 8.22 Hz, 1H), 3.03 (dd, *J* = 15.68, 0.60 Hz, 1H), 0.90 (s, 9H), 0.10 (s, 3H), 0.09 (s, 3H). ¹³C-NMR (150 MHz, CDCl₃): δ 200.46, 137.45, 128.88, 128.42, 128.11, 75.48, 73.21, 71.68, 56.42, 49.13, 43.51, 25.92, 18.25, −4.64, −4.96. HRMS–ESI: $[M + H]^+$ calcd. for $C_{19}H_{32}NO_3Si$: 350.2152; found 350.2142.

3.2.8. *tert*-Butyl (3*S*,4*R*)-4-(benzyloxy)-3-((*tert*-butyldimethylsilyl)oxy)azepane-1-carboxylate (**3e**)

To a solution of tetrahydroazepine **2** (75 mg, 170 μmol) in methanol (350 μL) was added 5% *w/w* Pd/C (2 mg, 1 μmol, 0.5 mol %). The suspension was then stirred under H₂ (1 atm) for 16 h until completion as confirmed by TLC. Catalyst was removed by passage through a plug of Celite with methanol rinsing. Solvent was then removed in vacuo to yield azepane **9** as a colourless oil (36 mg, 48%). $[\alpha]_D^{20}$ −200 (*c* 0.14, CHCl₃); FTIR (ATR): 2929, 2856, 1691, 1165, 1082, 834, 774 cm⁻¹. ¹H-NMR (400 MHz, CDCl₃): 7.40–7.23 (m, 5H), 4.70–4.55 (m, 2H), 3.93 (m, 0.5H), 3.87–3.54 (m, 3.5H), 3.20–3.00 (m, 2H), 2.05–1.94 (m, 1H), 1.85–1.69 (m, 1.5H), 1.68–1.57 (m, 1H), 1.56–1.38 (m, 9.5H), 0.95–0.88 (m, 9H), 0.13–0.05 (m, 6H). δ ¹³C-NMR (150 MHz, CDCl₃): δ 155.57, 139.54, 128.57, 127.65, 127.58, 80.39, 74.51, 72.30, 72.19, 50.06, 46.76, 28.89, 26.20, 26.20, 23.43, 18.44, −4.26, −4.38. HRMS–ESI: $[M + H]^+$ calcd. for $C_{24}H_{42}NO_4Si$: 436.2883; found 436.2875.

3.2.9. (3*S*,4*R*)-4-(Benzyloxy)-3-((*tert*-butyldimethylsilyl)oxy)azepan-1-ium (**4c**)

Azepane **3e** (5.0 mg, 11 μmol) was *N*-Boc deprotected as above for **3a**, yielding **4c** as a colourless oil (3.9 mg, quant.). $[\alpha]_D^{20}$ −84 (*c* 0.03, CHCl₃); FTIR (ATR): 2930, 2857, 1674, 1199, 1131, 834, 778 cm⁻¹. ¹H-NMR (400 MHz, CDCl₃): δ 10.12 (s, broad, 1H), 8.07 (s, broad, 1H), 7.40–7.26 (m, 5H), 4.67–4.51 (m, 2H), 4.22 (m, 1H), 3.66–3.52 (m, 1H), 3.32 (m, 2H), 3.16 (m, 2H), 1.98 (m, 2H), 1.80 (m, 2H), 0.89 (s, 9H), 0.086 (m, 6H). ¹³C-NMR (150 MHz, CDCl₃): δ 138.32, 128.79, 128.14, 127.94, 81.05, 72.42, 71.06, 47.28, 45.94, 26.71, 26.03, 20.97, 18.32, −4.41, −4.84. HRMS–ESI: $[M + H]^+$ calcd. for $C_{19}H_{34}NO_2Si$: 336.2359; found 336.2348.

4. Conclusions

Overall, we have shown here that the late-stage oxidation of tetrahydroazepine **2** constitutes an efficient way to access novel oxo-azepines. Hydroboration of **2** with BH₃·SMe₂ yielded azepanols **3a** and **3b** in a 3:2 product ratio and, following oxidation, afforded regioisomeric ketones **5a** and **5b**. Separation of these ketones was readily achieved to provide **5a** and **5b** in 29% and 19% overall yield, respectively. Regioselectivity can be improved by using additives such as Rh(COD)(DPPB)BF₄,

albeit with competitive hydrogenation (Table 3, Entry 4), to access ketones **5a** and **5b** in a 1:7 product ratio, over 8 steps and in 30% overall yield for **5b**. Azepanols **3a/b** and oxo-azepines **5a/b** are versatile synthons and, following complete deprotection, useful epitopes in the construction of novel azepane-based biological agents. As a point of comparison, the work of Spiegel et al. highlighted the synthetic utility of their C6 ketone **vi** in the concise synthesis of glucosepane via a sigmatropic rearrangement and cyclization sequence in a total of 13 steps and 12% overall yield from diacetone-D-glucose (Scheme 1b). Ketones **5a** and **5b** structurally resemble compound **vi** as trisubstituted oxo-azepines bearing a protected vicinal dihydroxyl motif with *syn* stereochemistry at C3 and C4. The availability of a more-efficient route may assist in future biological investigations focused on glucosepanes.

Author Contributions: H.S. and F.L. conceived and designed the experiments; H.S. performed the experiments and H.S., P.K. and F.L. analyzed the data. P.K. performed the DFT study and analyzed the data. H.S., P.K. and F.L. wrote the paper.

References

1. Bouquet, J.; Bleriot, Y.; Desire, J.; King, D.T.; Vocadlo, D.J.; Vadlamani, G.; Benzie, G.R.; Mark, B.L.; Iorga, B.; Ide, D.; et al. Selective Trihydroxylated Azepane Inhibitors of NagZ, a Glycosidase Involved in *Pseudomonas aeruginosa* Resistance to β-Lactam Antibiotics. *Org. Biomol. Chem.* **2017**. [CrossRef] [PubMed]

2. Basak, R.K.; Vankar, Y.D. Synthesis and Comparative Study of Homoisofagomines and Analogues as Glycosidase Inhibitors. *Eur. J. Org. Chem.* **2014**, *2014*, 844–859. [CrossRef]

3. Li, H.; Zhang, Y.; Favre, S.; Vogel, P.; Sollogoub, M.; Bleriot, Y. Synthesis of Branched Seven-Membered 1-*N*-Imino-Sugars and Their Evaluation as Glycosidase Inhibitors. *Carbohydr. Res.* **2012**, *356*, 110–114. [CrossRef] [PubMed]

4. Kalamkar, N.B.; Kasture, V.M.; Chavan, S.T.; Sabharwal, S.G.; Dhavale, D.D. Concise and Practical Route to Tri- and Tetra-Hydroxy Seven-Membered Imino-Cyclitols as Glycosidase Inhibitors from D-(+)-Glucurono-γ-Lactone. *Tetrahedron* **2010**, *66*, 8522–8526. [CrossRef]

5. Shih, T.-L.; Yang, R.-Y.; Li, S.-T.; Chiang, C.-F.; Lin, C.-H. Expeditious Synthesis of Tri- and Tetrahydroxyazepanes from D-(-)-Quinic Acid as Potent Glycosidase Inhibitors. *J. Org. Chem.* **2007**, *72*, 4258–4261. [CrossRef] [PubMed]

6. Parker, L.J.; Watanabe, H.; Tsuganezawa, K.; Tomabechi, Y.; Handa, N.; Shirouzu, M.; Yuki, H.; Honma, T.; Ogawa, N.; Nagano, T. Flexibility of the P-Loop of Pim-1 Kinase: Observation of a Novel Conformation Induced by Interaction With an Inhibitor. *Acta Crystallogr. Sec. F Struct. Biol. Cryst. Commun.* **2012**, *68*, 860–866. [CrossRef] [PubMed]

7. Yamashita, D.S.; Marquis, R.W.; Xie, R.; Nidamarthy, S.D.; Oh, H.-J.; Jeong, J.U.; Erhard, K.F.; Ward, K.W.; Roethke, T.J.; Smith, B.R. Structure Activity Relationships of 5-, 6-, and 7-Methyl-Substituted Azepan-3-one Cathepsin K Inhibitors. *J. Med. Chem.* **2006**, *49*, 1597–1612. [CrossRef] [PubMed]

8. Breitenlechner, C.B.; Wegge, T.; Berillon, L.; Graul, K.; Marzenell, K.; Friebe, W.-G.; Thomas, U.; Schumacher, R.; Huber, R.; Engh, R.A. Structure-Based Optimization of Novel Azepane Derivatives as PKB Inhibitors. *J. Med. Chem.* **2004**, *47*, 1375–1390. [CrossRef] [PubMed]

9. Cipolla, L.; Araújo, A.C.; Airoldi, C.; Bini, D. Pyrrolo [2,1-*c*][1,4] Benzodiazepine as a Scaffold for the Design and Synthesis of Anti-Tumour Drugs. *Anti Cancer Agents Med. Chem. Former. Curr. Med. Chem. Anti Cancer Agents* **2009**, *9*, 1–31. [CrossRef]

10. Rajanarendar, E.; Reddy, M.N.; Krishna, S.R.; Reddy, K.G.; Reddy, Y.; Rajam, M. Design, Synthesis, in vitro Antimicrobial and Anticancer Activity of Novel Methylenebis-isoxazolo[4,5-*b*]azepines Derivatives. *Eur. J. Med. Chem.* **2012**, *50*, 344–349. [CrossRef] [PubMed]

11. Smid, P.; Mlinaric, M.; Koehler, K.F.; Nunez Garcia, S.; Wegener, E.; Lange, J.H.M. Spiro Azepane-Oxazolidinones as Kv1.3 Potassium Channel Blockers. US8575148B2, 18 October 2010.

12. Uchikawa, O.; Sakai, N.; Terao, Y.; Suzuki, H. Preparation of Fused Heterocyclic Compounds as Apoptosis Signal Regulating Kinase 1 (ASK1) inhibitors. WO2008016131A1, 7 February 2008.

13. Anderson, K.W.; Fotouhi, N.; Gillespie, P.; Goodnow, R.A., Jr.; Guertin, K.R.; Haynes, N.-E.; Myers, M.P.; Pietranico-Cole, S.L.; Qi, L.; Rossman, P.L.; et al. Preparation of Pyrazole-4-Carboxamide Derivatives as 11-β-Hydroxysteroid Dehydrogenase Form I (11-β-HSD1) Inhibitors. WO2007107470A2, 27 September 2007.

14. Brummerhop, H.; Frick, W.; Glombik, H.; Plettenburg, O.; Bickel, M.; Heuer, H.; Theis, S. Synthesis of Fluoro-Glycoside Derivatives of Pyrazoles for Use in Treatment of Diabetes or For Lowering Blood Sugar Levels. WO2005121161A1, 22 December 2005.

15. Ammenn, J.; Gillig, J.R.; Heinz, L.J.; Hipskind, P.A.; Kinnick, M.D.; Lai, Y.-S.; Morin, J.M., Jr.; Nixon, J.A.; Ott, C.; Savin, K.A.; et al. Preparation of 1,3,4-Oxadiazoles and Related Compounds for Use as Melanin Concentrating Hormone Antagonists in the Treatment of Obesity and Diabetes. WO2003097047A1, 27 November 2003.

16. Hartman, G.D.; Kuduk, S. Preparation of Azepane Derivatives and Methods of Treating Hepatitis B Infections. WO2015109130A1, 23 July 2015.

17. Wilson, F.X.; Nash, R.J.; Horne, G.; Storer, R.; Tinsley, J.M.; Roach, A.G. Compounds, Including Alkaloids and Iminosugars, for the Treatment of Flaviviral Infections. WO2010015815A2, 26 August 2010.

18. Núñez-Villanueva, D.; Infantes, L.; García-López, M.T.; González-Muñiz, R.; Martín-Martínez, M. Azepane Quaternary Amino Acids As Effective Inducers of 3_{10} Helix Conformations. *J. Org. Chem.* **2012**, *77*, 9833–9839. [CrossRef] [PubMed]

19. Kamal, A.; Reddy, D.R.; Reddy, P.M.M. Synthesis and DNA-Binding Ability of Pyrrolo[2,1-*c*][1,4]benzodiazepine-Azepane Conjugates. *Bioorg. Med. Chem. Lett.* **2006**, *16*, 1160–1163. [CrossRef] [PubMed]

20. Johnson, H.A.; Thomas, N.R. Polyhydroxylated Azepanes as New Motifs for DNA Minor Groove Binding Agents. *Bioorg. Med. Chem. Lett.* **2002**, *12*, 237–241. [CrossRef]

21. Psarra, V.; Fousteris, M.A.; Hennig, L.; Bantzi, M.; Giannis, A.; Nikolaropoulos, S.S. Identification of Azepinone Fused Tetracyclic Heterocycles as New Chemotypes with Protein Kinase Inhibitory Activities. *Tetrahedron* **2016**, *72*, 2376–2385. [CrossRef]

22. Pellegrino, S.; Bonetti, A.; Clerici, F.; Contini, A.; Moretto, A.; Soave, R.; Gelmi, M.L. 1*H*-Azepine-2-oxo-5-amino-5-carboxylic Acid: A 3_{10} Helix Inducer and an Effective Tool for Functionalized Gold Nanoparticles. *J. Org. Chem.* **2015**, *80*, 5507–5516. [CrossRef] [PubMed]

23. Pellegrino, S.; Contini, A.; Clerici, F.; Gori, A.; Nava, D.; Gelmi, M.L. 1*H*-Azepine-4-amino-4-carboxylic Acid: A New α,α-Disubstituted Ornithine Analogue Capable of Inducing Helix Conformations in Short Ala-Aib Pentapeptides. *Chem. Eur. J.* **2012**, *18*, 8705–8715. [CrossRef] [PubMed]

24. Draghici, C.; Wang, T.; Spiegel, D.A. Concise Total Synthesis of Glucosepane. *Science* **2015**, *350*, 294–298. [CrossRef] [PubMed]

25. Andersen, S.M.; Ekhart, C.; Lundt, I.; Stutz, A.E. Syntheses of Sugar-Related Trihydroxyazepanes from Simple Carbohydrates and Their Activities as Reversible Glycosidase Inhibitors. *Carbohydr. Res.* **2000**, *326*, 22–33. [CrossRef]

26. Shih, T.-L.; Liang, M.-T.; Wu, K.-D.; Lin, C.-H. Synthesis of polyhydroxy 7- and *N*-alkyl-azepanes as potent glycosidase inhibitors. *Carbohydr. Res.* **2011**, *346*, 183–190. [CrossRef] [PubMed]

27. Otero, J.M.; Estevez, A.M.; Soengas, R.G.; Estevez, J.C.; Nash, R.J.; Fleet, G.W.J.; Estevez, R.J. Studies on the Transformation of Nitro-Sugars into Branched Chain Imino-Sugars. Part II: Synthesis of (3*R*,4*R*,5*R*,6*S*)-2,2-bis(hydroxymethyl)azepane-3,4,5,6-tetraol. *Tetrahedron Asymmetry* **2008**, *19*, 2443–2446. [CrossRef]

28. Dhavale, D.D.; Markad, S.D.; Karanjule, N.S.; PrakashaReddy, J. Asymmetric Dihydroxylation of D-Glucose Derived α,β-Unsaturated Ester: Synthesis of Azepane and Nojirimycin Analogues. *J. Org. Chem.* **2004**, *69*, 4760–4766. [CrossRef] [PubMed]

29. Dhavale, D.D.; Chaudhari, V.D.; Tilekar, J.N. An Expeditious Synthesis of a (3*S*,4*S*,5*R*)-Trihydroxyazepane. *Tetrahedron Lett.* **2003**, *44*, 7321–7323. [CrossRef]

30. Zamoner, L.O.B.; Aragao-Leoneti, V.; Mantoani, S.P.; Rugen, M.D.; Nepogodiev, S.A.; Field, R.A.; Carvalho, I. CuAAC Click Chemistry with *N*-Propargyl-1,5-dideoxy-1,5-imino-D-gulitol and *N*-propargyl 1,6-dideoxy-1,6-imino-D-mannitol Provides Access to Triazole-Linked Piperidine and Azepane Pseudo-Disaccharide Iminosugars Displaying Glycosidase Inhibitory Properties. *Carbohydr. Res.* **2016**, *429*, 29–37. [CrossRef] [PubMed]

31. Adams, C.; Fairway, S.; Hardy, C.; Hibbs, D.; Hursthouse, M.; Morley, A.; Sharp, B.; Vicker, N.; Warner, I. Total Synthesis of Balanol: A Potent Protein Kinase C Inhibitor of Fungal Origin. *J. Chem. Soc. Perkin Trans.* **1995**, 2355–2362. [CrossRef]

32. Fürstner, A.; Thiel, O.R. Formal Total Synthesis of (-)-Balanol: Concise Approach to the Hexahydroazepine Segment Based on RCM. *J. Org. Chem.* **2000**, *65*, 1738–1742. [CrossRef] [PubMed]

33. Goumain, S.; Taghzouti, H.; Portella, C.; Behr, J.-B.; Plantier-Royon, R. Convenient Strategy for the Synthesis of Highly Functionalizable Hydroxylated Unsaturated Azepanes. *Tetrahedron Lett.* **2012**, *53*, 4440–4443. [CrossRef]

34. Li, H.; Bleriot, Y.; Chantereau, C.; Mallet, J.-M.; Sollogoub, M.; Zhang, Y.; Rodriguez-Garcia, E.; Vogel, P.; Jimenez-Barbero, J.; Sinay, P. The First Synthesis of Substituted Azepanes Mimicking Monosaccharides: A New Class of Potent Glycosidase Inhibitors. *Org. Biomol. Chem.* **2004**, *2*, 1492–1499. [CrossRef] [PubMed]

35. Moutel, S.; Shipman, M.; Martin, O.R.; Ikeda, K.; Asano, N. Synthesis of a Trihydroxylated Azepane from D-Arabinose By Way of an Intramolecular Alkene Nitrone Cycloaddition. *Tetrahedron Asymmetry* **2005**, *16*, 487–491. [CrossRef]

36. Li, H.; Zhang, Y.; Vogel, P.; Sinay, P.; Bleriot, Y. Tandem Staudinger-azaWittig Mediated Ring Expansion: Rapid Access to New Isofagomine-Tetrahydroxyazepane Hybrids. *Chem. Commun.* **2007**, 183–185. [CrossRef] [PubMed]

37. Patel, A.R.; Ball, G.; Hunter, L.; Liu, F. Conformational Regulation of Substituted Azepanes Through Selective Monofluorination. *Org. Biomol. Chem.* **2013**, *11*, 3781–3785. [CrossRef] [PubMed]

38. Patel, A.R.; Hunter, L.; Bhadbhade, M.M.; Liu, F. Conformational Regulation of Substituted Azepanes through Mono-, Di-, and Trifluorination. *Eur. J. Org. Chem.* **2014**, *2014*, 2584–2593. [CrossRef]

39. Patel, A.R.; Liu, F. Diastereospecific Fluorination of Substituted Azepanes. *Tetrahedron* **2013**, *69*, 744–752. [CrossRef]

40. Corey, E.; Cho, H.; Rücker, C.; Hua, D.H. Studies with Trialkylsilyltriflates: New Syntheses and Applications. *Tetrahedron Lett.* **1981**, *22*, 3455–3458. [CrossRef]

41. Corey, E.; Venkateswarlu, A. Protection of Hydroxyl Groups as *tert*-Butyldimethylsilyl Derivatives. *J. Am. Chem. Soc.* **1972**, *94*, 6190–6191. [CrossRef]

42. *Molecular Operating Environment (MOE)*; 2016.08; Chemical Computing Group Inc.: Montreal, QC, Canada, 2016.

43. *TURBOMOLE*, V7.1; University of Karlsruhe and Forschungszentrum Karlsruhe GmbH: Karlsruhe, Germany, 2016.

44. Männig, D.; Nöth, H. Catalytic Hydroboration with Rhodium Complexes. *Angew. Chem. Int. Ed. Engl.* **1985**, *24*, 878–879. [CrossRef]

45. Evans, D.A.; Fu, G.C.; Hoveyda, A.H. Rhodium (I)-Catalyzed Hydroboration of Olefins. The Documentation of Regio-and Stereochemical Control in Cyclic and Acyclic systems. *J. Am. Chem. Soc.* **1988**, *110*, 6917–6918. [CrossRef]

46. Westcott, S.A.; Blom, H.P.; Marder, T.B.; Baker, R.T. New Homogeneous Rhodium Catalysts for the Regioselective Hydroboration of Alkenes. *J. Am. Chem. Soc.* **1992**, *114*, 8863–8869. [CrossRef]

47. Evans, D.A.; Fu, G.C.; Hoveyda, A.H. Rhodium (I)-and Iridium (I)-Catalyzed Hydroboration Reactions: Scope and Synthetic Applications. *J. Am. Chem. Soc.* **1992**, *114*, 6671–6679. [CrossRef]

48. Burgess, K.; Cassidy, J.; Ohlmeyer, M.J. Substrate-Controlled Diastereoselectivities in Catalyzed and Uncatalyzed Hydroborations of Acyclic Allylic Alcohol Derivatives: Secondary Orbital Effects Involving d.π-p.π. Interactions. *J. Org. Chem.* **1991**, *56*, 1020–1027. [CrossRef]

49. Burgess, K.; Ohlmeyer, M.J. Diastereocontrol in Rhodium-Catalyzed Hydroboration of Chiral Acyclic Allylic Alcohol Derivatives. *Tetrahedron Lett.* **1989**, *30*, 395–398. [CrossRef]

50. Harder, S.; Spielmann, J. Calcium-Mediated Hydroboration of Alkenes: "Trojan horse" or "True" Catalysis? *J. Organomet. Chem.* **2012**, *698*, 7–14. [CrossRef]

51. Crudden, C.M.; Edwards, D. Catalytic Asymmetric Hydroboration: Recent Advances and Applications in Carbon-Carbon Bond-Forming Reactions. *Eur. J. Org. Chem.* **2003**, *2003*, 4695–4712. [CrossRef]

52. Beletskaya, I.; Pelter, A. Hydroborations Catalysed by Transition Metal Complexes. *Tetrahedron* **1997**, *53*, 4957–5026. [CrossRef]

53. Burgess, K.; Ohlmeyer, M.J. Transition-Metal Promoted Hydroborations of Alkenes, Emerging Methodology for Organic Transformations. *Chem. Rev.* **1991**, *91*, 1179–1191. [CrossRef]

54. Carroll, A.-M.; O'Sullivan, T.P.; Guiry, P.J. The Development of Enantioselective Rhodium-Catalyzed Hydroboration of Olefins. *Adv. Synth. Catal.* **2005**, *347*, 609–631. [CrossRef]

55. Yamamoto, Y.; Fujikawa, R.; Umemoto, T.; Miyaura, N. Iridium-Catalyzed Hydroboration of Alkenes with Pinacolborane. *Tetrahedron* **2004**, *60*, 10695–10700. [CrossRef]

56. Lata, C.J.; Crudden, C.M. Dramatic Effect of Lewis Acids on the Rhodium-Catalyzed Hydroboration of Olefins. *J. Am. Chem. Soc.* **2009**, *132*, 131–137. [CrossRef] [PubMed]

57. Noh, D.; Chea, H.; Ju, J.; Yun, J. Highly Regio-and Enantioselective Copper-Catalyzed Hydroboration of Styrenes. *Angew. Chem. Int. Ed. Engl.* **2009**, *48*, 6062–6064. [CrossRef] [PubMed]

58. Noh, D.; Yoon, S.K.; Won, J.; Lee, J.Y.; Yun, J. An Efficient Copper (I)-Catalyst System for the Asymmetric Hydroboration of β-Substituted Vinylarenes with Pinacolborane. *Chem. Asian J.* **2011**, *6*, 1967–1969. [CrossRef] [PubMed]

Sample Availability: Samples of the compounds are not available from the authors.